Anna Bevià Brey

Porous alumina-based electrochemical biosensor for bovine mastitis detection

Final Degree Project

Supervised by Dr. Beatriz Prieto Simón

Co-supervised by Deepanshu Verma

Degree in Biomedical Engineering

Tarragona

September 2023

ACKNOWLEDGEMENTS

First of all, I would like to emphasize the sincere gratitude I feel towards Professor Beatriz Prieto, who, given the circumstances, showed from the very beginning the flexibility, interest and confidence in helping me to carry out this project. A thesis that began to take shape at the beginning of November and that has gone through a process of assimilation throughout the course until today.

In the same way, to recognize the effort and constancy of Deepanshu Verma. He played a key role in designing the frameworks for this project and provided me with the guidelines, the essential tools, and a constant support to ensure its successful execution.

I would also like to express my gratitude to the entire research team for the kindness and welcoming in their interactions with me, making me feel part of all of them. For me it has been really valuable to learn about the dynamics of a scientific research group, and to observe the significance of the collaboration among professionals from different fields of expertise with a common research objective.

I wish to express the indispensable suport extended by my entire family. Right from the onset, they have expressed interest in understanding the subject, the scope and the evolution of my research endeavours.

Lastly, I would like to underscore how meaningful studying Biomedical Engineering degree at URV has been for me. By concluding this academic stage, I can honestly say that I have discovered a captivating field with so many domains and applications. It also gave me the opportunity to connect with a great group of people with whom I've shared classes, experiences and common interests throughout these four years, culminating in an extraordinary phase of personal and professional growth.

INDEX

1. INTRODUCTION.

1.1. Presentation of the project.

Within the realm of science, when confronted with a pathological condition, the ability of formulating a precise diagnosis becomes evident. The unequivocal identification of the responsable agent for the morbid symptoms and manifestations together with the information collated by specialized medical professionals enable judicious and tailored therapeutic interventions.

At present, diagnostic determinations primarily derive from the symptomatic profile exhibited by the patient. However, certain maladies commence evincing symptomatic traits during the advanced phases of their progression, thereby often impeding the timely identification and implementation of efficacious therapeutic protocols. The diagnostic process entails a comprehensive scrutiny of the patient's symptomatic manifestations, coupled with the assimilation of suitable data collected by specialized medical personnel.

Consequently, the early-stage detection of ailments conferes advantageous outcomes for the afflicted individual while bypasses temporal constraints. This early-stage disease detection paradigm holds potential utility across both human and animal domains, showing up as a robust and potent diagnostic instrument.

The following project aims to study and review the bases and mechanisms of early detection of bovine mastitis linked to the discovery, research, application, and use of reliable biomarkers present in infected cow’s milk. This aim will be achieved through the development of analytical devices capable of detecting key biomarkers for the diagnosis of bovine mastitis.

Available data reveals there are aproximately 300 million dairy cows worldwide, yielding an anual milk output of approimately 600 million tons. The European Union stands as the largest milk producer globally. Importantly, the viability of milk production in dairy herds rests with good udder health [1].

Bovine mastitis is among the most common and challenging diseases in the worldwide dairy industry. Mastitis is an inflammation of the parenchyma of the mammary glands/udder of bovines [2], due to physical damage, chemical irritation, or in most cases, because of an infection caused by bacterial pathogens, chiefly *Escherichia coli* and *Streptococcus uberis* [3]. It is considered to be a harmful condition for dairy herds, affecting animal well-being and supposing huge economically incurring losses to the dairy industry through decreased production and milk quality standards, a decline of farm profitability, increase in processing and animal treatment costs, and the boost on the herds culling rates when high rates of infection are identified within the herd [4]. Diagnosis of the causative agents of mastitis is often not performed, with treatment being applied to veterinary predefined protocols. The strategies for managing mastitis

encompass the administration of systematic or intrammamary antibiotics as soon as possible aiming to both treat and preempt the disease, with a pronounced emphasis on addressing the heightened risk of antibiotic resistance [19].

In this context, the early diagnosis of bovine mastitis is of utmost importance. On the one hand, the prompt diagnosis could help to reduce the use of antibiotics in the field of livestock farming. This is key beacuse the missuse and/or overuse of antibiotics may have a negative impact on animal's immune response and on human health by inducing antibiotic-resistant pathogens that may spread and end up in milk. On the other hand, prompt diagnosis can easen the growing social concern about the conditions in which animals are kept in farms. This is highly relevant because of the pressure of animal welfare and the ethical, cultural and emotional considerations that derive from it, are now more than ever, in the spotlight. Without setting aside, the economic impact that results from [8]. In addition, mastitis affects the compositon of milk, and the degree of changes depends on the infecting agent and the inflammatory response, which cannot be used for human purposes due to its altered chemical composition and organoleptic properties [19]. Thus, prompt diagnosis is key to avoid the affected milk reaches the consumers.

Today, bovine mastitis management approaches revolve around measures aimed at averting disease. These measures encompass special attention to farm hyigine protocols and trained personnel. Skilled professionals have to discern subtle alterations in cow's udder or milk's quality and consitency, as often clinical mastitis is detected by farmers via visual inspection of the inflammation. While disease prevention remains imperative, the development of early-stage detection tools utilizing advanced diagnostic strategies and terapeutic protocols, even not being developed yet, assume presedence in the realm of medical research [7][8]. The present project reviews how the early diagnosis of bovine mastitis can be reached through the detection of key biomarkers present in milk.

Biomarker is a term used within the realm of biochemistry, to describe specific molecules that serve as reliable indicators of health and existence of a disease. These molecules are present in various bodily fluids of both human and animal organisms such as milk. Biomarkers are detected and quantified through the utilization of specific laboratory tools and procedures [5].

MiRNA is a biomolecule that meets most of the requiered characteristics for being an ideal biomarker. It can be detected and quantified through minimally invasive procedures in easyly accessible bodily fluids, ideally before the clinical symptoms appearance. Its sensitive detection can be translatable from research to clinical procedures [6]. MiRNA role is gene regulation by mediating the degradation of mRNA and by regulating transcription and translation, and intercellular signalling. Since mastitis significantly compromises the expression levels of inflammation-related miRNAs in bovine milk, these stand as potential biomarkers for the early diagnosis of bovine mastitis [6]. Specifically, miRNA-223, upon others such miR-26a, miR-142, miR-

146a, has been frequently reported to be upregulated in milk or milk components in association with bovine mastitis [1].

Recognizing the significance of developing an early diagnostic tool and comprehending the future's study potential, the main objective of this study is to develop a point-of-care device capable of detecting miRNA–223 in milk, a key host immune-derived biomarker upregulated in the milk of infected cows for the early bovine mastitis diagnose. MiRNA-223 is comprissed within a complex matrix comprising diverse cellular constituents, encompassing lipids, proteins, and other biomolecules. The efforts are focused on extending biosensing while minimizing matrix effects when working with milk samples.

1.2 Sensing platform.

In a world landascape marked by the growing emergence of diseases, it becomes evident that the proper identification, monitorning and treatment of these ailments poses significant challenges. A thorough understanding of these challenges is crucial to mitigate and counteract the spread of diseases in a prompt manner, preventing their potential outcomes from painting an excessively bleak picture.

In the context of bovine mastitis diagnosis, distinct methods can be distinguished. On farm, the quantification of somatic cell count in milk is the standard method, which is used to assess the likeliness of milk to contain harmful bacteria [9]. In the lab, both PCR and cell culture are used to ascertain mastitis and the causative pathogen. Lab methods are good in identifying the disease, the respective infectious agents and antibiotic resistent phenotypes. However, none of the descrived techniques, eventually, permits in-situ available data neither the promt stage diagnosis of the disease, which is when animals are highly infective and therapies are more effective [19]. Emergent diagnostic methodologies are being developed to effectively discern bovine mastitis during its nascent stages, thereby favoring timely and efficient intervention in the pursuit of expeditiously identifying the most suitable treatment. These evolving procedures are designed to detect specific biomarkers within milk samples, providing indicative insights of the initial cow's immune response [13].

Electrochemical Biosensor Technology appears today as a forefront tool when identifying infection causing pathogens, conferring advantageous outcomes in terms of rapid response, high sensitivity and selectivity, cost-effectiveness and ease of miniaturization [10][14]. Electrochemical sensors generate an electrochemical signal, which can be transduced into a readable electric signal, when interacting the target analyte on the electrode surface. When specific biomolecules are immobilized on the surface of the electrode, they specifically interact with the target analyte, converting the analyte binding into a measurable electric signal, which can be used to detect and quantify the target analyte [11][17]. The first electrochemical biosensor was developed

to detect glucose in blood. Since then, a wealth of electrochemical biosensors have been designed and developed for analytes of interest in a wide range of applications [12].

A miRNA-223 sensor appears as a of pioneering biosensing technology that has already been developed and further optimised that so far demonstrated its efficiency in detecting the target analyte in buffer. The present study reports the challenge aim of demonstrating its potential to reliably detect miRNA-223 in milk for bovine mastitis diagnosis through non-invasive and stress-free milk biopsies [13].This pursuit strives to certify the viability of the biosensor in detecting specific bovine mastitis-related biomarkers as precise and specific agents to perform an effective and timely staged diagnosis early recognition of the targeted ailment.

The interest for developing an electrochemical biosensor for the early diagnosis of bovine mastitis arises from the multiple advantages of electrochemical biosensing over other techniques. For this specific application, electrochemical biosensors offer the possibility of delivering real-time information on cow's health status by measuring directly in milk, without causing any disturb neither stress tp the animals. As a result, farmers can monitor their herds in real time and easily spot and adress any issue that may require prompt attention and intervention, which is imperative for timely-stage diagnosis. The biosensor has to be designed according to its intended function, in this specific case being portable and easily miniaturized which empowers it to be well-suited for point-of-care scenarios, to be freely used in-situ, bypassing the need to gather samples and perform laboratory testing. Likewise, electrochemical biosensors should be developed under cost-effective conditions, harnessing easily accessible materials [10] [13].

To design an electrochemical biosensor for bovine mastitis diagnosis, the first step requires the identification of the target analyte. As previously discussed, miRNA-223 was selected in this work as a key host immune-related biomarker present in milk. Advances in biosensing technology make possible to design the sensor that better fits to the specific function they are intended to perform, together with the characteristics of the biomarker and the type and location of the sample to be used for the analysis. In this project a biosensor built on porous anodic aluminum oxide-based sensor (pAAO) is selected as the basis for the sensing platform. The sensing mechanism of the pAAO biosensor consists on measuring pore blockage caused upon hybridization of the target analyte to the capture probe. The decision to use pAAO as the basis platform, was made on the one hand, aiming to maximise the sensitivity of miRNA levels when using a sensing mechanism based on pore blockage, and thus, to detect tiny concentration of miRNA. On the other hand, striving to overcome matrix effects from milk, which are known to be one of the limiting steps when developing a sensor. Minimise interferences can be achieved thanks to the possibility to tune pore morphology. The selection of the

pAAO platform and the implementation of a sensing mechanism based on pore blockage have been specifically tailored to resolve these two identified issues.

pAAOs exhibit a large surface area-to- volume ratio resulting in a large reactive surface area, thereby enchancing sensitivity. Likewise, the sensing mechanism based on pore blockage upon miRNA hybridization to the immobilized capture probe also contributes to reach heightened sensitivity. Furthermore, morphological attributes of the porous material play significant importance when minimizing the issues related to matrix effects. In the context of the present study, pAAO biosensors have been presicely selected as the basis for the sensing platform, which can be specially tailored to meet the specific sensing requierements.

While the primary aim of developing pAAO-based adresses disease diagnosis, the potential to identify the causative pathogen poses a challenge of significant importance. This can be achieved by further developing pAAO sensor into an array of sensors targeting a panel of key miRNA. This approach enables the specific identification of pathogens. However, milk has a broad range of bacteria, and bovine mastitis does not stem from the presence of a single specific bacterium. So bovine mastitis identification has to consider multiple factors.

2. Material and Methods.

The objective of the present work is to fabricate a customized biosensor for DNA sensing, serving as an initial step towards designing a miRNA sensor. The use of porous anodic aluminium oxide (pAAO) as the substrate serves as the basis for the biosensor development, encompassing multiple enchained steps.

1. Fabrication of Porous alumina
    a. Pre-treatment of aluminium substrate.
    b. Electropolishing.
    c. First Anodization.
    d. Etching of un-ordered pores.
    e. Second Anodization.
    f. Chemical etching of aluminium.
    g. Barrier oxide layer removal.
2. Functionalization
    a. Hydroxylation.
    b. Silanization.
    c. Carboxylation.
    d. DNA conjugation
    e. Surface blocking.

3. Electrochemical techniques
    a. Cyclic Voltammetry basic principles.
    b. Electrochemical impedance spectroscpy principles.
    c. Square wave voltammetry principles.
    d. Electrode activation.
    e. Stability measurements.
4. Experimental conditions.

2.1. Fabrication of porous alumina (pAAO).

In recent years, and due to an exponential biomedical growing demand, there has been an increase in both the necessity and interest surrounding the development of highly sensitive biosensor devices. Special attention has been paid in developing biosensors by using readily accessible nanomaterials. Tailored biosensors are deployed under self-ordered synthesis via electrochemical anodization. Those are not only cost effective, and easy-reproducible but also distinguished by their extensive physical and chemical attributes compared to other conventional techniques. Their unique properties have made them a distinctive tool of immense potential in the biosensor development and production framework.

The fabrication of pAAO through electrochemical anodization includes the oxidation of aluminum when immersed inside an electrolyte solution, giving rise to the formation of highly ordered, and well vertically aligned pores. The resulting pAAO substrates possess unique properties that when prepared as membranes, can simulate protein nanochannels in cell membranes in a well reproducible manner. If they are modified with suitable receptors, they can offer distinct single molecule sensitivity and selectivity. Furthermore, according to the sensing requirements of the present study, parameters including size and width of the pore can be modified to enhance the aimed sensing [15].

To comprehend the mechanism behind the electrochemical anodization of aluminium, each metallic element exposed to atmospheric oxygen, as illustrated in Equation 1.1, or aqueous media, in accordance with Equation. 1.2, undergoes an oxidation process. Oxidation leads to a shift from simple oxides to elaborated compounds. This reaction takes place spontaneously since it is thermodynamically favoured by the negative Gibb's free energy change. On a molecular level, this mechanism involves electron loss by the metal, increasing the oxidation state. Likewise, on a physical level, a thin layer of the metal oxide is formed on the outermost layer [15].

$$2Al\ (s) + \frac{3}{2}O_2\ (g) \rightarrow Al_2O_3\ (s) \qquad \Delta G^{\circ} = -1582\,\frac{\mathrm{KJ}}{\mathrm{mol}} \qquad Eq.1.1$$

$$2Al\ (s) + \ 3H_2O\ (l) \rightarrow Al_2O_3\ (s) + + 3H_2(g) \qquad \Delta G^{\circ} = -871\,\frac{\mathrm{KJ}}{\mathrm{mol}} \qquad Eq.1.2$$

2.1.1. Pre-treatment of aluminium substrate.

High-purity aluminium sheets, particularly 99.999% pure aluminium foils with a 0.5 mm thickness, obtained from Goodfellow Cambridge Ltd., are earmarked for the fabrication of pAAO membranes. In preparation for the anodization process, the aluminium samples undergo a series of pre-treatment steps to ensure optimal surface conditions.

Firstly, the aluminum sheets are meticulously cut into 2 cm x 2 cm squares, ensuring uniform sample sizes and smooth surface. This is necessary to achieve consistent pAAO film in the following anodization process. Subsequently, the aluminum squares are carefully cleaned with successive ethanol 96% v/v and water washes to eliminate potential contaminants that may affect the anodization process. Moreover, to ensure the removal of any oil or grease trace, the aluminium squares are degreased with acetone. It is crucial to emphasize the flatness of the aluminum samples. Obtaining a flat surface is essential for achieving a uniform and consistent pAAOa film during the subsequent anodization process.

2.1.2. Electropolishing process.

After the execution of the pre-treatment step, the 2x2 cm^2 aluminium substrates are placed in the PVC cell, wherein they will be exposed to the electrolyte solution. Upon successfully positioned the samples, the PVC cell and the bottom copper plate are screwed together with aluminium samples carefully clamped in between them.

The electropolishing process consists of the application of a constant voltage of 20 V for a duration of 6 minutes, which direction is switched under regular stirring. This voltage triggers the outermost layer ions dissolution when the metal is immersed in the electrolyte solution, composed by aqueous perchloric acid solution. The execution of the electropolishing practice is eased using a specialized software which already contains the set parameters to induce the process.

In order to understand the process of ion dissolution, aluminum is designated as the anode, which is linked with the positive terminal of the voltage generator. Contrarly, the cathode typified by the platinium wire of the cell, is connected to the negative terminal of the voltage generator. Both the anode and the cathode are immersed within the electrolyte solution. It is within this environament that it is observed the electrical motion between the anode and the cathode, which prompts the dissolution of the aluminium most superficial layer ions. Thus, after the electropolishing procedure is achieved, a marginal and insignificant reduction in the surface of the aluminum piece is obtained. Resulting in a consistent, clean and shiny surace finish. The visual difference between the bare aluminium before and after the electropolishing process is evidenced in both Figure 1.A and Figure 1.B.

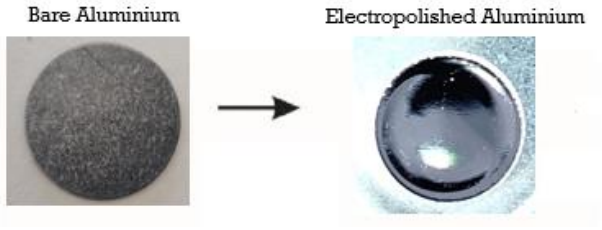

Figure 1.(A) Piece of bare aluminium, (B) Electropolished aluminium.

2.1.2. First anodization process.

Upon succesfully completing the electropolishing process, and obtaining a pristine and impurity-free aluminium substrate surface, the piece is subjected to the first anodization process. The process results in the formation of highly ordered and regular pore arrays within the alumina layer.

pAAO can be fabricated using different electrolytes to obtain different pore sizes and densities, to achieve specific sensing requirements. Each electrolyte solution has specific conditions of use.

- Anodization in 0.3 M sulphuric acid results in obtaining pores of between 15-20 nm. Consists of applying a regular voltage of 20 V at 5°C.
- Anodization in 0.3 M oxalic acid is used if 30-35 nm pores are sought. Requires invariable voltage of 40 V at 5°C.
- Anodization in 1% phosphoric acid is used to achieve the largest pore size, of about 90-100 nm. Likewise, the aluminium is subjected to a potential of 175 V to form an oxide passivation layer which helps avoiding the breakdown of the pAAO layer formed under hard anodization condition at 195 V and -5°C.

Under the framework of this study, 0.3 M oxalic acid is used to perform the first anodization process to obtain highly ordered and regular 30-35 nm pore arrays within the pAAO layer. The execution of the first anodization is set at 40 V for a period of 20 hours under constant stirring. The procedure is facilitated by a specialized software that encompasses all parameters of interest. Over the last decades, the study of the anodization parameters has led to exhaustive comprehension of how they affect pAAO's attributes. Notably, those variables including electrolyte composition and concentration, voltage, and temperature have been identified as key parameters. Thus, influencing the process of pore self-organization and giving them the resultant geometrical attributes [16].

Once the voltage is switched on, O^- ions from the electrolyte move towards the aluminum plate – anode - . Contrarly, aluminum ions move in the opposite direction towards the cathode. This electronic exchange results in a oxidation reaction that gives rise to the formation of a thin and compact aluminum oxide layer on the outermost alumium stratum. Thus, pure aluminum becomes Al_2O_3 [14] [15].

Until now, the exhibited aluminum material had properties of high conductivity. Yet the newly oxidized compound is no longer so, as the conductivity attribute is drastically reduced. The conductivity graph certifies how during the early stages of the anodizing process, the current density undergoes a severe fall as described in S1 Figure 2, which corresponds to the growth of the layer of Al_2O_3 on the aluminum's surface. Along the process, the electrolytic interchange persists and trigger instabilities across the oxide barrier layer. Progressively, the conductive capacity is slightly recovered but in a very discrete way, as illustrated in S2 and S3, Figure 2. Eventually, when the ion concentration at opposing sides is balanced, the current density takes a stable value, as discerned in S4, Figure 2 [15].

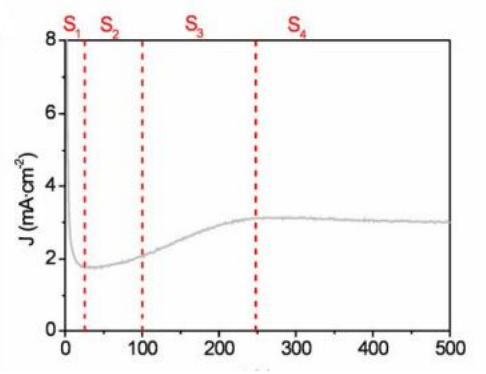

Figure 2. Graph showing the different stages of pore formation [14].

Simultaneously to the described S1 stage, the application of a constant voltage between the anode and the cathode, coupled with the ion motion, gives rise to imprimts on the primary surface of the thin and compact Al_2O_3 layer. These impressions appear without breaching the layer, as evidenced in Figure 3.B These patterns mark the early beginning where the subsequent development of pores will unfold, by electronic exchange [14] [15].

Concurrently to the evidenced S2 phase, wherein the conductivity pharameter exhibits marginal recover, the persistent electronic exchange induces instabilities within the electric field that dissolve localy the oxide material. Thus, inducing the formation of nucleation centers for the subsequent pore growth, as displayed in Figure 3.C. Throughout the continuous ion movement, instabilities persistently dissolve nucleation centers, leading to a gradual perforation of the Al_2O_3 layer. Therefore, nanopores progressively develop, as portrayed in the following Figure 3.D and Figure 3.E. This would correspond to the slightly recovery of conductivity as seen on S3 and the reaching of the asymptote value represented in the S4 curve on Figure 2. At the end of the first anodization process, the result is an aluminium matrix full of a complex assemblage of disorderly, irregular, and hexagonal pores, as evidenced in both Figure 4.A and Figure 4.B [14] [15].

.

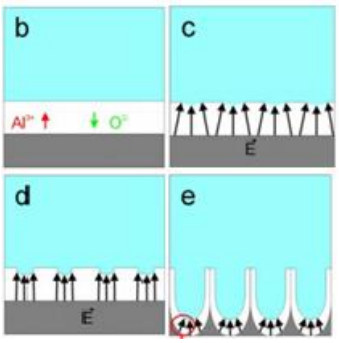

Figure 3. Formation of nucleating centers [14].

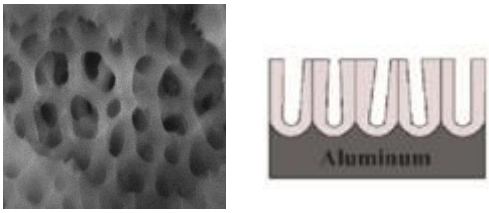

Figure 4 (A) SEM image of the top view of an alumina substrate after the first anodization, (B) Schematics depicting the cross-section view of the pores after the first anodization.

When examinating the nanopore structure, chemically, two main regions can be distinguished. The first one corresponds to the innermost layer of the pore, comprising predominantly pure alumina. In contrast, the second region represents the outermost position, located between the innner layer and the alumina-electrolyte, as it is revealed by Fig 5. This domain becomes contaminated by anionic species coming from the acid electrolyte [15].

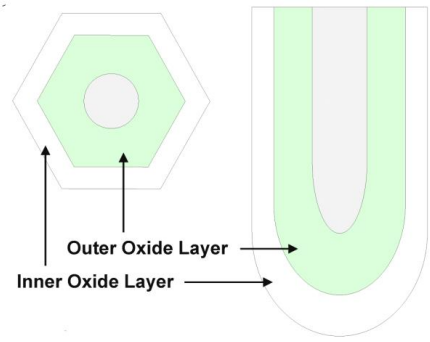

Figure 5. Modified image showing the chemical structure of the pore, top and cross-sectional views [15].

2.1.3. Etching: removal of unordered pores.

Between the first and the second anodizing process there is an intermediate chemical etching. This step consists on the removal of the unordered pAAO film obtained during the first anodization. The resulting pure aluminium template with the indentations will give rise to ordered pores in the second anodization process.

To achieve this, it is necessary to properly clean the cell and the samples with deionized water, followed by washing with ethanol 96% v/v . Then, they are finally dried using compressed air. To proceed with the chemical etching, an acid solution composed of 85% phosphoric acid (H_3PO_4) and ≤98% chromic acid (H_2CrO_4) is used. Each sample is left to rest in this solution at 70°C for 60 minutes at a constant stirring of 450 rpm. Then the alumina substrates are washed with deionized water and dried with compressed air.

After the etching step, unordered pores have been removed, and ordered concatives are formed at the nucleation centers from first anodization. Showing a shape very similar to the one observed in Figure 6. The template is now ready to perform a second anodization to guide the new pores growth in a ordered and regular way.

Figure 6. Schematics depicting the cross-section view of the nucleative centers formed after removal of unordered pores.

2.1.4. Second anodization process.

According to the first anodization, in the second anodization, the samples undergo a thorough cleaning procedure using deionized water and ethanol 96% v/v. After that, they are dried and carefully clamped in the cell. A MATLAB program is then selected, which operates at the same voltage as the first anodization, 40 V. However, unlike before where pore thickness was controlled by time, now the key anodizing parameter to be set is the total accumulated charge of the electrochemical system. Throughout the execution of the process, the electronic interchange favours the aluminium consumption, as noticed in the scheme of Figure 7 [15].

Figure 7. Schematics depicting the cross-section view of the pores after the 2nd anodization process.

When fabricating pAAO using 0.3 M oxalic acid and 0.3 M sulphuric acid, a total charge of 2.27 C/cm^2 is sought to achieve a growth of 1 µm of thickness. In contrast, when using 1% phosphoric acid, 1.49 C/cm^2 is necessary to reach the same thickness growth. Then, to obtain the total charge to apply it is necessary to run the following calculation: charge to apply (C) x number of samples x sought height (µm). In the context of this study, a

total heigh of 30 µm is expected, as samples have been tailored in previous experiments according to the specific sensing requirements. The meticulous oversight of the applied charge is key to achieve consistent procedures and reproducible results [15].

After the completion of the second anodizing process, a comparable matrix to the one obtained after the first anodizing is obtained. Nevertheless, the significant difference arises in the fact that the pore structure now shows a neat and systematic ordered arrangement [15].

2.1.5. Etching: removal of the aluminium and barrier oxide layer.

The porous film generated on the aluminium surface resulting from the second anodization process is not yet suitable for biosensing applications. The reason is the need of a pAAO membrane with a through-hole morphology, accordingly to the specific context of use [15].

After the second andodization process is done, the following step consists of the aluminium and oxide barrier layer removal to obtain free-standing pAAO membranes, i.e. open pores [15].

The first step involves the oxidation of the aluminium, wich is the material present on top of the pAAO film. A solution made of copper chloride ($CuCl_2$) and hydrochloric acid (HCl) is used to succesfully get rid of the aluminium. Once the aluminium from the back side of the pAAO film is completely etched, a barrier type aluminium oxide layer is exposed, with a pattern that follows similarly to the displayed Figure 8.

Figure 8. Schematics depicting the cross-section view of the pores after aluminium layer removal.

The samples are then thoroughly cleaned with deionized water and then clamped carefully in a custom-built teflon cell. The removal of the aluminium exposes the underlying barrier oxide layer, which is located underneath. The displayed oxide barrier layer is then immersed in 5% phosphoric acid at 55°C for 25 minutes inside an incubator. This process opens the barrier layer at the pore bottom to achieve a through-hole morphology of the pAAO membrane, as despicted in the Figure 9.

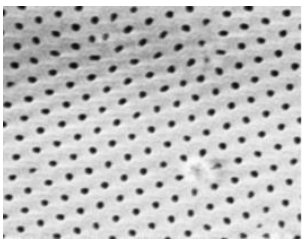

Figure 9. SEM image of the top view of a pAAOs structure taken after aluminium and barrier oxide layer removal.

2.2. Surface modification.

The functionalization step consists of introducing functional groups on the obtained pAAO membranes to prepare them for their further biosensing uses, as despicted on Figure 10. So far, the membranes show hexagonal and ordered pores on their surface, but they haven't been yet prepared for the covalent binding with the chosen bioreceptors [16]. Bioreceptors are those molecules that specifically identify and interact with the target analyte. The immobilization of the bioreceptor inside the pAAO pores is only achieved by proper membrane functionalization [17] [18].

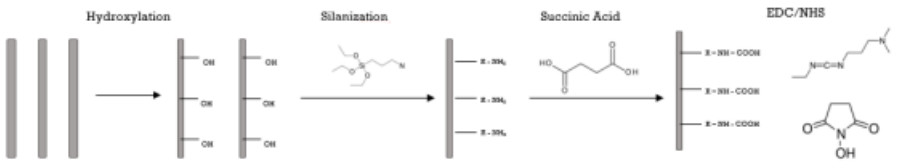

Figure 10. Surface modification processes of pAAOs membranes showing hydroxilation, silanization, succinic acid and EDC/NHS.

2.2.1. Hydroxylation.

The previously treated membranes are first cleaned with deionized water and ethanol and then placed in a schlenk flask, filled with H_2O_2. The flask is then placed inside a preheated oil bath at 180°C-200°C. The pAAO membranes are boiled in H_2O_2 for 45 minutes. The tube is sealed with a rubber stopper and a needle is placed in order to facilitate vapours release. After that, the membranes are dried carefully with nitrogen and they are kept in the oven at a temperature of 60 °C for two hours, as they need to be totally dry. After this step is done, OH groups are expected on the pAAO's surface. An oil bath is used, as this has a very high boiling temperature.

2.2.2. Silanization.

Following the incorporation of -OH groups onto the surface, the pAAO substrates are meticulously transferred to a teflon holder positioned within a Schlenk flask. This flask is then hermetically sealed using a rubber stopper to uphold a controlled environment and establish an inert atmosphere. The initiation of the silanization process entails the injection of 99.85% extra dry toluene into the flask via a syringe, while simultaneously maintaining a continuous nitrogen flow at a consistent temperature of 28°C. The wet-chemical silanization method is used in a moisture-free space. It involves using a solution of (3-aminopropyl) triethoxysilane (APTES) dissolved in dry toluene (5% v/v) for about 30 minutes. Once the silanization step is done, the substrate is taken out and washed with toluene to remove any leftover chemical residues. Following this, the membranes are placed in an oven and dried for a period of 1 hour at 100°C. Finally, the dried membranes are carefully stored under vacuum conditions until further use. After this step, amine (NH_2) groups are obtained on the pAAO's surface.

2.2.3. Succinic acid.

Succinic acid provides two carboxyl groups. One of which will bind to the NH_2 groups on the pAAO surface, and the other will bind to the NH_2 group linked to the capture probe, in this study, an NH_2-modified -single stranded DNA (5'-NH2-C6-AGTTATCCCAGTCTTATAGGTAGGT-3')-. Following the successful incorporation of amines by functionalizing the membranes using APTES, the subsequent stage encompasses carboxylation to establish CO-NH_2 bonds, thereby leaving an available COOH group for future functionalization. To execute carboxylation, a solution of succinic acid in dimethyl sulfoxide (DMSO) is used at a concentration of 0.2 M. Succinic acid, being a dicarboxylic acid, comprises two carboxylic acid functional groups (-COOH). The amine groups, stemming from the APTES functionalization and present on the membrane surface, interact with the carboxylic acid group (-COOH) of succinic acid molecules, resulting in the generation of CO-NH_2 bonds. This chemical reaction is recognized as amide bond formation.

Throughout the carboxylation process, the COOH groups from succinic acid are effectively affixed onto the amine-functionalized membrane surface, thus introducing novel functional groups. Those new introduced COOH groups serve as reactive sites for subsequent functionalization pursuits. The available COOH group facilitates the subsequent bonding of specific bioreceptors. This approach enables the anchoring of desired bioreceptors onto the membrane surface.

2.2.4. Carbodiimide activation.

Two solutions are prepared for the functionalization process. The first solution comprises 10 mg/mL N-(3-dimethylaminopropyl)-N'-ethylcarbodiimide hydrochloride (EDC) , while the second solution consists of 15 mg/mL N-hydroxysuccinimide (NHS). These solutions are combined in a 1:1 (v/v) ratio in 0.1 M MES buffer, adjusted to a pH of 5.4. The pAAO substrates, which have previously undergone the carboxylation procedure, are now meticulously arranged within a petri dish. Over each substrate, the EDC-NHS solution is precisely poured, ensuring comprehensive coverage across the surface. To enhance kinetics of the reaction, the petri dish is positioned on a shaker, allowing the reaction to progress for a duration of 30 minutes. In this phase, EDC and NHS molecules present in the solution interact with the carboxyl groups on the pAAO membrane surface, thereby creating activated intermediates, which serve as reactive sites for subsequent conjugation reactions and favouring the attachment of biomolecules such as ssDNA.

2.2.5. Incubation with DNA capture probe.

The EDC-NHS chemistry employed in this study is well-known for its effectiveness in activating carboxyl groups for conjugation purposes. This chemical allows the modification of the pAAO membranes with specific biomolecules featuring amine groups. In the context of study, pAAO sensors are incubated with 100 µL of a 0.5 µM solution of ssDNA capture probe (5´-NH2-C6-TGGGGTCAAACTGACA-3´) prepared in 0.1 M phosphate buffered saline (PBS). Likewise, for controls a volume of 0.5 µM solution of a random ssDNA sequence (5'-NH2-C6-AGTTATCCCAGTCTTATAGGTAGGT-3') prepared in 0.1 M PBS is used. This random sequence is selected to ensure no hybridization to the target analyte occurs. Then, the samples are left to rest on a sheaker for a period of 1 hour at room temperature followed by overnight on the fridge at a temperature of 3-4ºC.

2.2.6. Ethanolamine.

Each sensor undergoes in this step, a meticulous incubation procedure involving ethanolamine. Since ethanolamine is used as a blocking agent, ensures surface blocking by saturating any unreacted sites remaining on the pAAO surface. The utilization of ethanolamine serves to reduce non-specific binding, thereby enchaning the specificity of subsequent analyte binding events. A volume of 300 µL of 0.1 M ethanolamine, prepared in 0.1 M phosphate-buffered saline (PBS) at a pH of 7.4, is used for each sensor. This incubation process is carried out in a shaker with periodic agitation, for a duration of 1 hour at ambient temperature.

2.3. Electrochemical techniques.

pAAOs biosensor mechanism involves the measurement of partial pore blockage that occurs when the analyte is recognized by the capture probe. When DNA hybridation occurs, the pores show partial blockage that can be cuantified through the use of electrochemical techniques involving redox species into the reaction. This is the reason to use a ferro/ferricyanide solution. Ferro/ferricyanide helps in the oxidation current of the redox species in the measurement solution diffusion towards the screen-printed electrode surface. Providing thus, a quantifiable measure of pore blockage.

Various electrochemical techniques are used to characterize the developed biosensors and to detect the target analyte in the sample to be analyzed. All techniques are used under faradaic conditions, so an electroactive species has to be added to the measuring solution. A 2 mM ferricyanide solution prepared in PBS at pH 7.4 is used. Such solution is made up of equimolar levels of ferrous ions (Fe^{2+}) and ferric ions (Fe^{3+}). These ions, present in aqueous solutions subjected to specific electrochemical potentials, demonstrate a propensity to engage in reduction and oxidation reactions. Preserving their balanced concentrationsions it's key, as it ensures a reciprocal relationship between the reduction and the oxidation proccesses, thereby facilitating the complete conversion of reduced species into oxidized counterparts and vice versa.

Within the ambit of study, the investigation of electrochemical phenomena has been facilitated by diverse electrochemical methods which have been deployed through the use of a tailor-made 3-electrode electrochemical teflon cell. This electrochemical setup encompasses the incorporation of a porous anodic aluminium oxide (pAAO) substrate. PAAOS serves as the substrate for sensing, affixed onto a C-SPE, which is used as the active working electrode. Likewise, the electrochemical configuration includes a platinium (Pt) counter electrode, and an Ag/AgCl reference electrode, both of them completing the experimental configuration framework.

2.3.1. Cyclic voltammetry basic principles.

Cyclic voltammetry is a commonly used electrochemical technique implemented to determine the reduction potential of a species within a solution when subjected to a specific voltage. The applied voltage undergoes changes over time, and the resulting current is tracked via a circuit comprised of an electrolyte cell, a working electrode where the redox reaction occurs, a counter electrode which operates in the reverse, and a reference electrode with a known potential.

Firstly, a potential considerably more positive than the redox species is applied, which ensures the complete oxidation of the species of interest, leading to the appearance of the first peak depicted in Figure 11. Subsequently, the potential is reversed in the negative direction, which progressively decreases the potential of the working electrode until it becomes negative relative to the redox species, thus initiating a reduction

reaction. Eventually, the voltage sweep is reversed, moving in the positive values until it returns to its initial configuration. This alternation in potential is carried out multiple times during a measurement, resulting in the characteristic shape of the cyclic voltammogram. As shown in Figure 11, this graph illustrates the relationship between current and applied voltage, revolving around current, as the voltage hits a threshold that induces a reduction or oxidation, prompting the flow of current [21] [22] [23].

To achieve the an accurate sensing, SWV parameters are set as follows: Estart -initial potential- of -0.2 V, Eends -final potential- of 0.8 V, a Estep -potential step- of 5 mV, one cycle of the square wave pulse, a current range of 100 µA, a square wave frequency of 5 Hz, and a pulse amplitude of 25 mV.

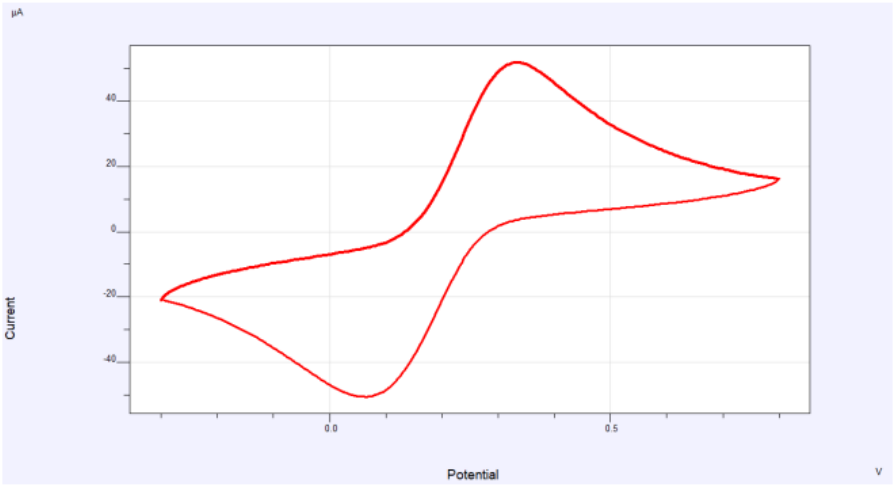

Figure 11. Cyclic voltammogram example including the main parameters to be considered: oxidation and reduction potentials (V) and intensity current values (µA).

2.5.2. Electrochemical impedance spectroscpy principles.

Electrochemical Impedance Spectroscopy (EIS) appears as a powerful tool developed to be used in the effective quantitative and qualitative biorecognition events occurring at the electrode surface. By applying a low-amplitude alternating current (AC) signal, EIS enables the analysis of cell impedance characteristics. Unlike single-frequency measurements, this technique enables the characterization of the electrochemical system through the sinusoidal application of multiple frequencies, followed by the acquisition of an impedance spectrum, as shown in Figure 12. This spectrum provides valuable insights into surface phenomena, changes in bulk properties, as well as exchange and diffusion processes. All this data is collected and used to generate a Nyquist plot, which is fitted to the theoretical model of the Randles circuit in order to determine parameters such as the charge transfer resistance (Rtc). In the framework of study, measurements take some specific values: Estart is set at 0.2 V, at 51 multiple frequencies, and the current range is confined at 100 µA.

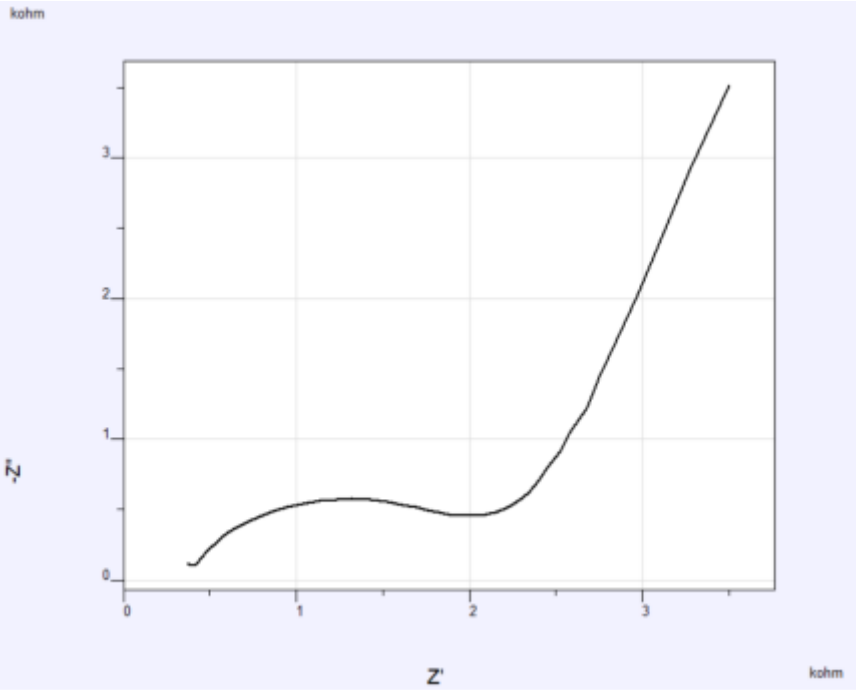

Figure 12. Electrochemical impedance spectropy spectrum example of imaginary impedance (Z'' - kohm) vs real impedance (Z' -kohm).

2.5.3. Square wave voltammetry principles.

Square wave voltammetry is a comprehensive technique that combines the benefits of cyclic voltammetry, pulse techniques, and impedance techniques, utilizing substantial amplitude variations. Considered to be one of the most sensitive pulse voltammetry techniques, according to the minmized contribution of the charging current replacing the continuous potential ramp of cyclic voltammetry shown on Figure 13. A, with a staircase potential-time depicted in Figure 13.B. During each wave cycle, the measured current is sampled twice: once at the conclusion of the direct potential pulse and again at the culmination of the inverse potential pulse, in both instances, just before the potential direction changes. This dual current sampling per square wave cycle yields two distinct current waveforms. The potential waveform, as observed in Figure 14, can resemble a superposition of a standard square wave atop an underlying scale [27] [28].

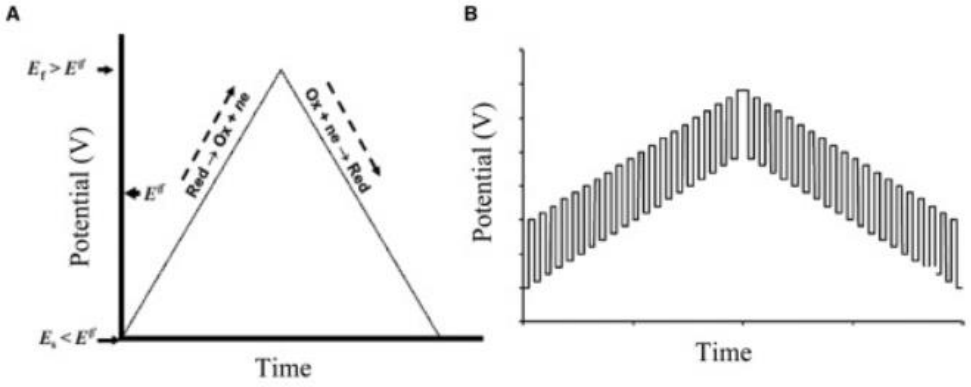

Figure 13. Modified image showing the change made on current analysis [29].

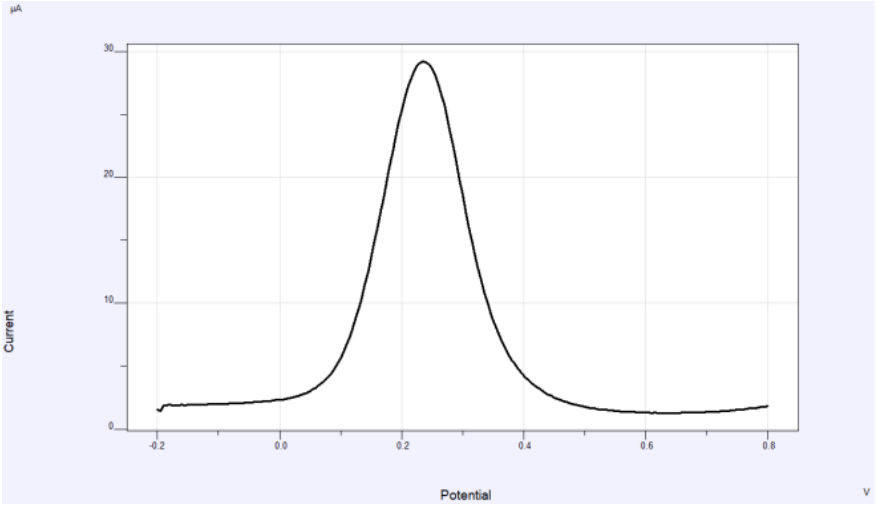

Figure 14.Square wave voltammogram example.

When observing them individually, the forward and reverse current waveforms mimic the appearance of a cyclic voltammogram as shown on Figure 14 and Figure 15.

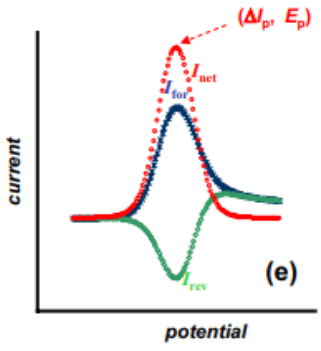

Fig 15. Cyclic voltammetry wave-form [27].

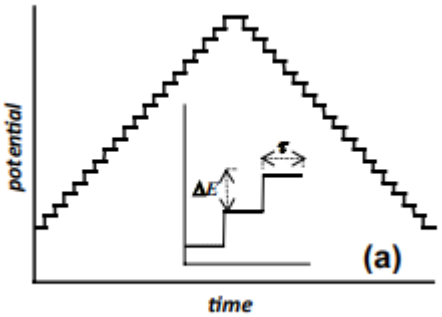

Fig 16. Cyclic voltammetry staircase plot [27].

In each cathodic pulse, there is a sudden reduction of the remaining analyte on the surface of the working electrode. Similarly, in each anodic pulse, the analyte that is previously reduced undergoes oxidation. The utilization of this technique offers several advantages. Firstly, the distinct signal of each pulse provides enhanced detail. Additionally, the peak's shape enables improved differentiation of adjacent signals, and the overall measurement process is expedited, thus increasing efficiency.

Throughout these procedures, the rationale behind the utilization of a minimally exposed surface area for the working electrode is to restrict the region wherein the reaction takes place. This deliberate confinement facilitates a clear observation of the targeted population of species under study [27].

The conditions used for SWV are E start = -0.2 V, E ends = 0.8 V, E step = 5 mV, 1 cycle, 100 µA of current range, SQRWV frequency = 5 Hz and 25 mV of pulse amplitude.

2.4. Electrode activation.

Commercial carbon-based screen-printed electrodes (C-SPEs) are used as electrochemical transducer of the biosensor, where pAAO membranes are deposited on top. SPEs are made of carbon-conductive ink. This ink composition comprises some non-conductive elements that can occasionally affect the electrochemical performance. Attempting to enhance electron transfer characteristics and thereby improve later the sensitivity to target compounds, some pre-treatment strategies have been devised. One such strategy involves an electrochemical activation treatment, consisting on applying a constant potential in repetitive cycles for a short period of time [29].

In this study, C-SPE electrodes from Quasense are activated by applying a potential of 1.2 V for 45 seconds to the C-SPE immersed in a 0.05 M carbonate buffer solution at pH 9.6. Following each amperometry cycle, cyclic voltammetry (CV) is performed in a 2 mM ferrocyanide and 2 mM ferricyanide solution prepared Ph 7.4 PBS. The third cyclic voltammogram for each step is recorded both before activation and after each activation cycle. Activation cycles are repeated until cyclic voltammograms from two consecutive activation steps exhibited similarity, indicating successful electrode activation.

2.5. Stability measurements.

Stability measurements are done to achieve a stable baseline signal from the sample electrodes. The electrochemical measurements are performed using a custom-built 3-electrode electrochemical teflon cell. The electrochemical cell comprises of a pAAO substrate as sensor platform, carbon screen-printed electrode as working electrode, a Pt counter electrode, and a Ag/AgCl reference electrode.

For stability measurements, up to 5 cycles of cyclic voltammetry, electrochemical impedance spectroscopy and square wave voltammetry are recorded with incubation of approximately 30 minutes between each measurement. The electrochemical measurements are performed in an 730 µL electrolyte solution of 2 mM $K_4[Fe(CN)_6]$ and 2 mM $K_3[Fe(CN)_6]$ prepared in 0.1 M PBS. The sensors are considered stable when at least 2 consecutive measurements show similar shapes with each other.

After reaching the stability, the aluminium samples ara properly washed and incubated with different concentrations of the target ss-DNA (5'- TGTCAGTTTGACCCCA -3): 0.1 pM, 1 pM, 10 pM, 100 pM and 1000 pM. After incubating for 30 minutes, CV, EIS and SWV are performed.

2.6. Experimental conditions.

The primary aim of this experiment is to ascertain the true efficacy of the already developed and optimised electrochemical miRNA-233 biosensor. However, Experimental conditions relate to a DNA sensor, which is used as a model of the RNA sensor to be developed. The reason to work with a synonim molecule relies in the fact that working with RNA is extremely sensitive due to the high inestability, and the elevated storage degradation rates while working with it. The single-stranded DNA used simulates the role of the RNA molecule but without compromising the experiment. Therefore, it is advisable to first test the effectiveness of the procedure before moving on to work with miRNA.

MiRNA-223 biosensor has already demonstrated its efficiency in detecting the target analyte in buffer. The objective is now to qualitatively examine milk samples and certify its potential in detecting miRNA-223 in milk. To that purpose, different experimental parameters have been defined, anchored in the evaluation of two samples: 0.1% milk and 0.1% double centrifuged milk incubated in increasing time periods. 5 different target analyte concentrations are analysed: 0.1 pM, 1 pM, 10 pM, 1000 pM and 1000 pM. Likewise 3 sensors and 3 controls of each concentration are used to have enough information to compare the results within the diferent conditions.

2. RESULTS.

The imperative of the study lies in the timely detection of bovine mastitis. Early diagnosis is key to make prompt decisions on whether cows need to be treated. The emergence of bovine mastitis, despite its multifaceted etiology, is most commonly attributed to pathogenic infection. This pathogen, recognized as exogenous within the host's organism, triggers an immune response, engendering discernible alterations in the expression and concentration of specific molecules, readily discernible in milk samples. The identification and quantification of biomarkers assume a pivotal role in comprehending the disease's essence, status, and progression. Moreover, this process contributes to uncovering the disease's underlying mechanisms and offers insights for selecting appropriate and personalized treatment strategies. Consequently, the design of sensing instruments, in this study exemplified by electrochemical biosensors, necessitates a framework equipped to analyze milk-based biological specimens and conduct meticulous detection, quantification, and analysis [19]. MIRNA-223 sensor has already been developed and demonstrated its efficiency in detecting the target analyte in buffer. The present work aims to demonstrate its potential in reliably detect miRNA in milk samples.

Recognizing the crucial significance of choosing an apt biomarker, the study has focused on miRNA-223. This microRNA holds a pivotal role in bovine mastitis detection, primarily due to its involvement in shaping the host immunological response and inflammation. Notably, miRNA-223 exhibits a distinct increase in expression as a response to the pathogenic factors underlying bovine mastitis [1].

Milk samples were obtained directly from bovines. Milk encompasses a mixture of solid and liquid components, comprising cells, fats, proteins, and assorted biomolecules. It's noteworthy that the inherent variability across milk samples compomises the matrix effects and the sensivity, since miRNA levels are low. Conversely, a centrifuged milk sample denotes one that has undergone prior separation, partitioning the denser solids which accumulate at the base, where biomarkers often aggregate, from the liquid constituents composing the supernatant. Furthermore, the use of the buffer at the experimental level assumes vital importance, as it has already been comproved its functioning, serving as a reference for gauging the basal signal in the absence of the interferint species. In this study, buffer is useful to compare results against diluted samples and to further assess matrix effects. This process substantiates the viability and functionality of the bespoke biosensor design. In essence, by comparing results in buffer and in diluted milk, wether centrifuged or not, matrix effects are assessed.

In order to conduct result readings, two electrochemical techniques have been selected: EIS and SWV. EIS is responsible for measuring the Rtc which is a suitable parameter to quantify miRNA hybridisation. Rtc measures the increasing resistance to charge transfer when larger amounts of miRNA analyte hybridise to the immobilised capture probe.

As for SWV, it measures the oxidation of the redox species within the ferrocyanide measuring solution. Consequently, reduced current values are indicative of the distinct presence of biomarkers in the studied sample.

All the results to be shown relate to a DNA sensor as a model of the RNA sensor to be developed and optimised, given the susceptibility within RNA molecules.

- **Analytical performance of the DNA sensor in buffer:**

It is imperative to reaffirm the pivotal role of assessing first the analytical performance of the sensor in buffer to later be able to assess mateix effects. The results obtained from both EIS and SWV measurements are crucial in comprehending the genuine functionality of the biosensor, as they facilitate the establishment of the expected sensor response in the absence of milk. As observed in Figure 17.A, particularly in the context of EIS, an increase in analyte concentration ideally should correspond to a discernible, bounded, and visual escalation in Rct values. There is an increasing obstruction to the diffusion of redox species that causes the charge transfer resistance to escalate. Conversely, Iox values measured via SWV indicate how the sensors, as despicted in Figure 17.B, with increasing analyte concentration, should gradually and parallelly diminish in alignment with the controls, which peak values are expected to remain stable as no DNA analyte binding is foreseen.

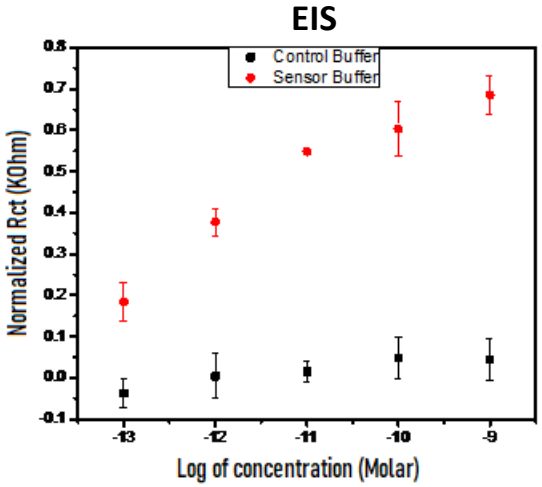

Figure 17.A. Detection obtained from EIS measurements performed in buffer.

.

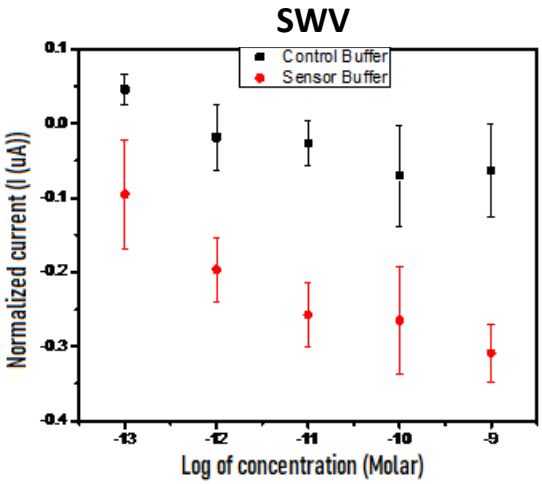

Figure 17.B. Detection obtained from SWV measurements performed in buffer.

As seen on the previous figures, EIS considers the Rtc against the concentration of target DNA sequence. Contrarly, SWV contemplates Iox against the increasing concentrations of target analyte. It's important to note that both Rtc and Iox parameters have been normalized. In the case of Rtc : {Rct(sample) - Rct(baseline)}/ Rct(baseline). Being Rtc beseline the reading of the blank value obtained after stability measurements without incubation with the target. Iox normalization consists on : {Iox(sample) – Iox (baseline)}/ Iox (baseline). Normalization is an essential step for the proper comparison and interpretation of results, as it enables the comparison of outcomes under different conditions.

- **Analytical performance of the DNA sensor in 0.1% milk:**

Next, the sensor is challenged against the detection of the analyte in milk to assess potential matrix effects. A 1000-fold milk dilution in PBS buffer is selected. Observations drawn from both EIS (Figure 18.A) and SWV (Figure 18.B) plots show how none of the concentrations shows a response significantly different between sensors and controls.

From a visual standpoint, no discernible differences can be observed between the sensors and control groups. Consequently, it becomes imperative to proceed with a statistical analysis of the results in an attempt to discern any underlying patterns. These outcomes exhibit a notable lack of repeatability, likely attributable to significant matrix effects.

The 0.1% milk sample comprises numerous cellular constituents within its composition, which have the potential to exert substantial influence on analytical readings. These cellular elements may introduce interference or disrupt the calibration process. One plausible approach to mitigating the matrix effects entails pretreating the milk sample through a dilution procedure, as described below.

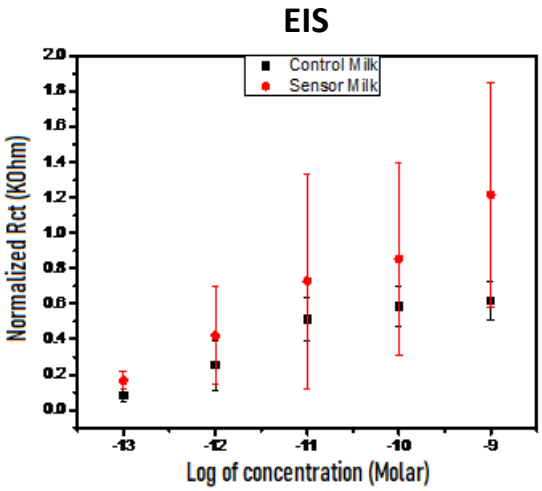

Figure 18.A. Detection obtained from EIS measurements performed in milk 0.1%.

Understanding the mechanism of the Randle circuit and the Warburg diffusion element, Rtc appear to be an useful tool to quantify miRNA hybridisation as it measures the increasing resistance to charge transfer when larger amounts of miRNA hybridise to the immobilised capture probe.

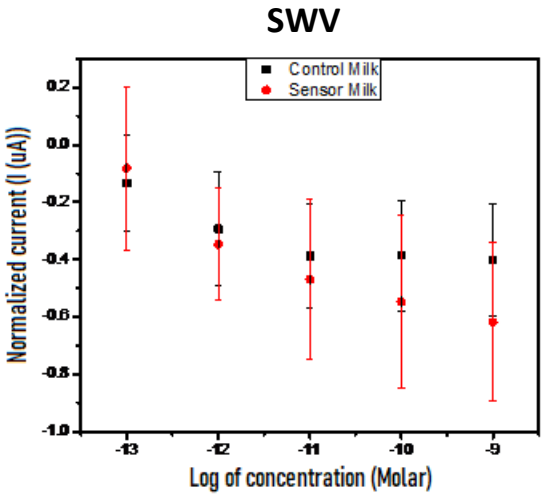

Figure 18.B. Detection obtained from SWV measurements performed in milk 0.1%.

- **Analytical performance of the DNA sensor in 0.1% double-centrifuged milk:**

With the aim of minimising the matrix effects previously observed, a milk pretretament step was applied prior to milk dilution. Such pretreatment consists of centrifuging milk two times. The interpretation of the calibration curve obtained from EIS results, shown in Figure 19.A, reveals a progressively heightened growth in Rct, indeed aligning with the ascending concentration of the sample. Despite the seemingly consistent outcomes, it is crucial to underscore the substantial variability inherent to the sensors, which in turn gives rise to a significant margin of error. Once again, it is noteworthy that the

variability intrinsic to the milk poses a formidable challenge in attaining precise and reproducible results.

However, the calibration curve depicting Iox values obtained from SWV measurements vs analyte concentration, shown in Figure 19.B, depicts coherent readings with a notably minor margin of error. Within this Figure, a gradual decrease in Iox is observed for sensors, mirroring the trend exhibited by the control samples, due to non specific adsorption of some milk constituents.

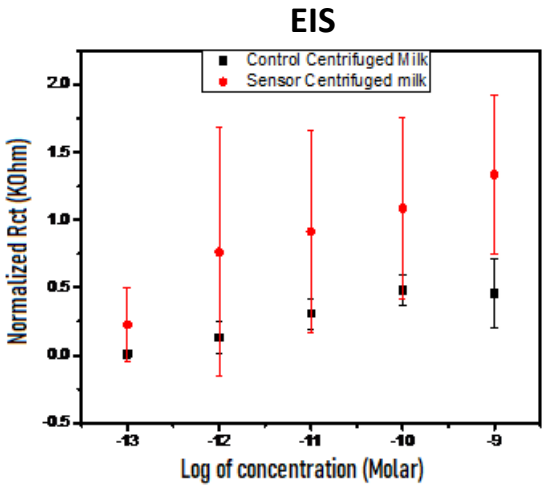

Figure 19.A. Detection obtained from EIS measurements performed in double-centrifuged milk 0.1%.

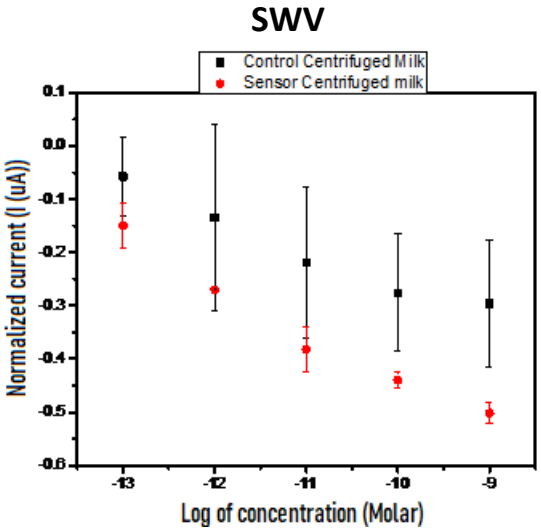

Figure 19.B. Detection obtained from SWV measurements performed in double-centrifuged milk 0.1%.

- **Results discussion**

While reviewing the EIS obtained data (Figure 20.A, 20.B), notably the increase in Rct values associated to control sensors tested in buffer samples is quite discreet yet those tested in both diluted and double centrifuged milk samples undergo a noticeable bounded growth in Rct. This trend is more significant when testing 0.1% milk samples. However, a stability pattern emerges starting from 100 pM, which is identified in both diluted, and centrifuged plus diluted milk samples, and could potentially be a result of the non-specific binfing of milk proteins to the sensor surface. This could indicate the onset of a process known as passivation, where a non-conductive or inhibitory surface layer forms on the sensor, blocking its response. This layer can restrict the transfer of charge. In the context of the 0.1% milk sample, especially at higher analyte concentrations, passivation might occur due to the absorption of milk components onto the sensor surface. As these components increase alongside milk incubation time, they contribute to the formation of a layer that hinders electron transfer and the desired electrochemical reaction.

Substantive variations in the extent of this growth, whether approaching exponential or otherwise, could plausibly be attributed to the substantial intrinsic variability to working with milk samples. Each specimen is liable to possess a subtly distinct compositional profile, thereby contributing to the observed deviations in growth patterns.

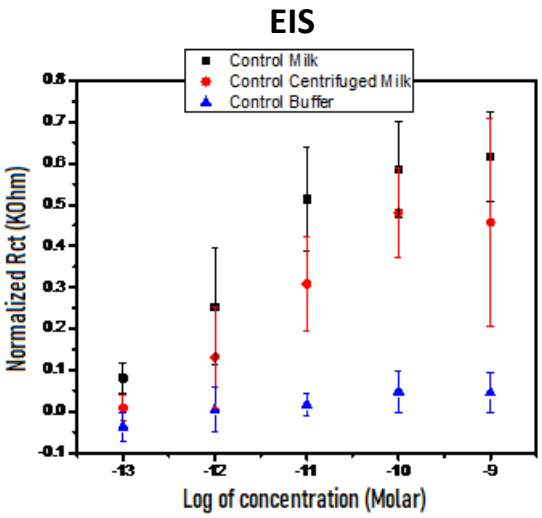

Figure 20.A. Detection obtained from EIS measurements performed between controls.

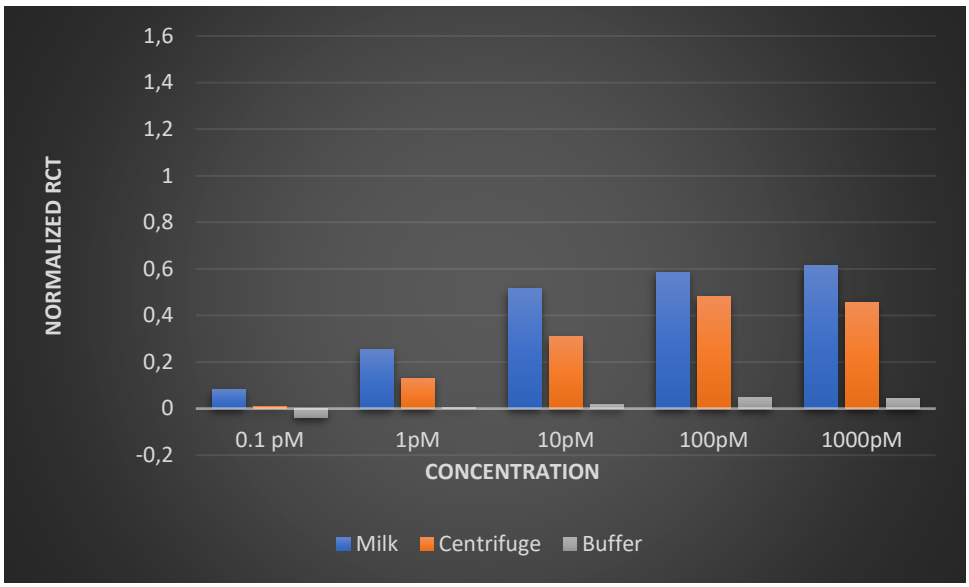

Figure 20.B. Bar chart comparing normalized Rct values against DNA concentrations obtained from EIS measurements using control sensors prepared.

The analysis of the reponse of controls measured from SWV (Figure 21.A, 21.B) shows there is a noticeable change in Iox values among the different samples. Starting with analyte solution prepared in buffer, as shown in Figure X, there is a gradual but marginal decrease in the current. Moving on to the centrifuged milk sample, as expected, there is a reduction in current, but this change is accompanied by a wide range of variability among controls within the same concentration. The most pronounced decrease in Iox is observed for the analyte solutions prepared in 0.1% milk. This trend aligns with the expectations and corresponds with the results seen for EIS results shown in Figure Y. Likewise, following the same pattern as for EIS analysis, some passivation is discerned, as after the concentration of 10 pM in 0.1% milk, the current value remains stable and does not change.

There is a signal decrease related to the adsorption of undesired compounds. The ideal and reliable results correspond to the lack of response for controls. Taking this as a patern it's possible to discern how the buffer performs well, but both milk 0.1% and double centrifuged 0.1% samples deviate from there. Centrifuged samples have some removed constituents that might contribute to the non-specific adsorption observed, so the effect now on the signal measured is less pronounced than for milk samples that have been just diluted.

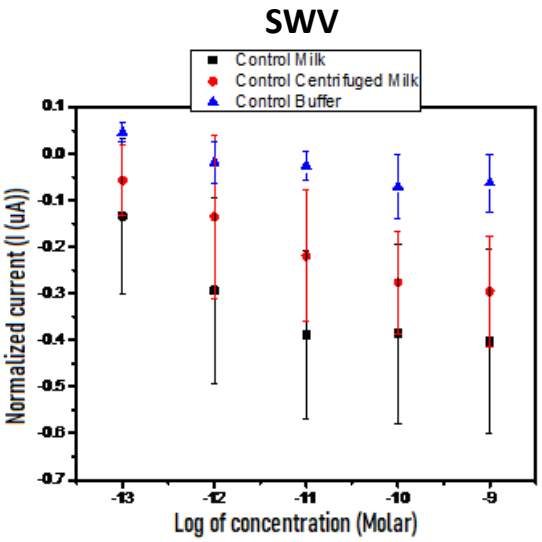

Figure 21.A. Detection obtained from SWV measurements performed between controls.

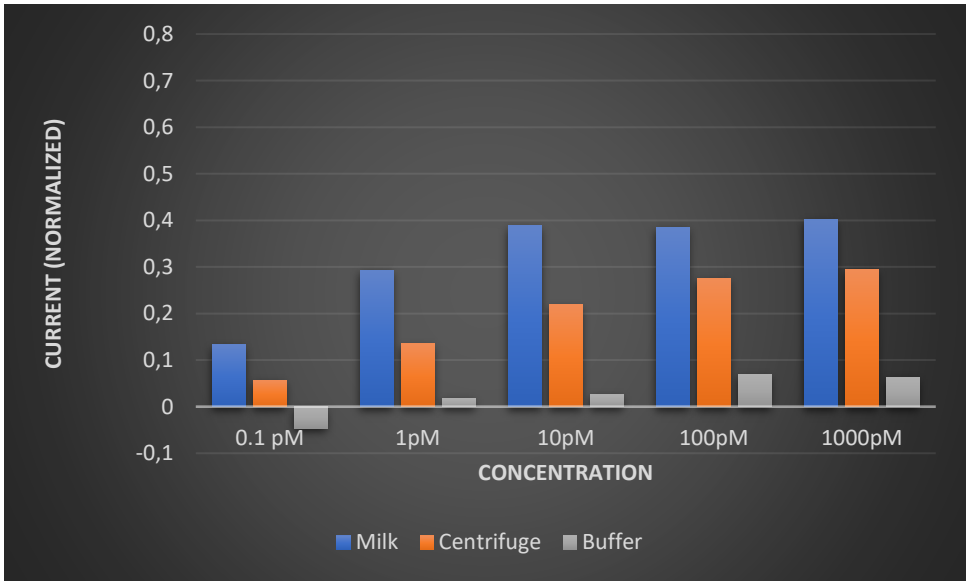

Graph 21.B. Bar chart comparing normalized Iox values against DNA concentrations obtained from SWV measurements using control sensors prepared.

While comparing the calibration curves obtained from EIS measurements using controls tested in buffer, 0.1% milk, and centrifuged and diluted milk, as shown in Figure 22.A, Figure 22.B, a discernible pattern emerges. Notably, the controls tested in buffer exhibit lesser variability in the outcome readings in comparison to milk and centrifuged milk samples. This congruence aligns with expectations, given there is no non-specific adsorption expected in buffer, as it does not include the target analyte. A gradual yet soft escalation in Rct is manifested. Turning attention to the milk samples, a more conspicuous growth is evident. This observation is consistent with the hypothesis that milk samples harbor a complex matrix comprising porteins, fats and other biomolecules. Thereby being prone to passivate the sensor and thus hinder charge transfer. Particularly noteworthy is the conspicuous growth observed

in the 0.1% milk sample. This specimen, characterized by its untreated nature and enriched composition of lipids, proteins, and diverse biomolecules, accentuates the pronounced growth phenomenon of resistance to the flow of current passage. Comparing the Rct values measured using controls and sensors, it is evident that the Rct calcualted at each concentration is now significantly higher, as the miRNA target biomolecule hybridises to the immobilised capture probe, causing significant pore blockage and thus affecting Rct.

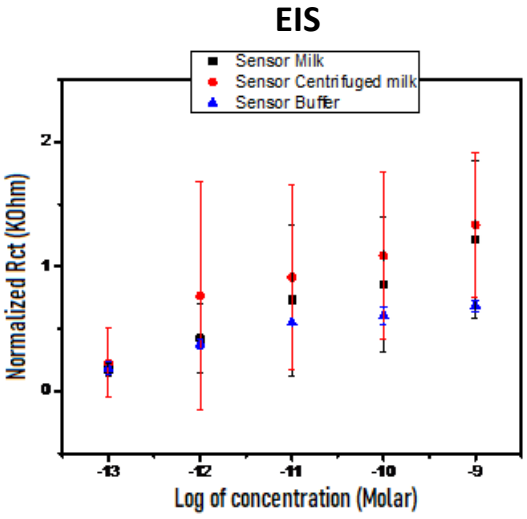

Figure 22.A. Detection obtained from EIS measurements performed between sensors.

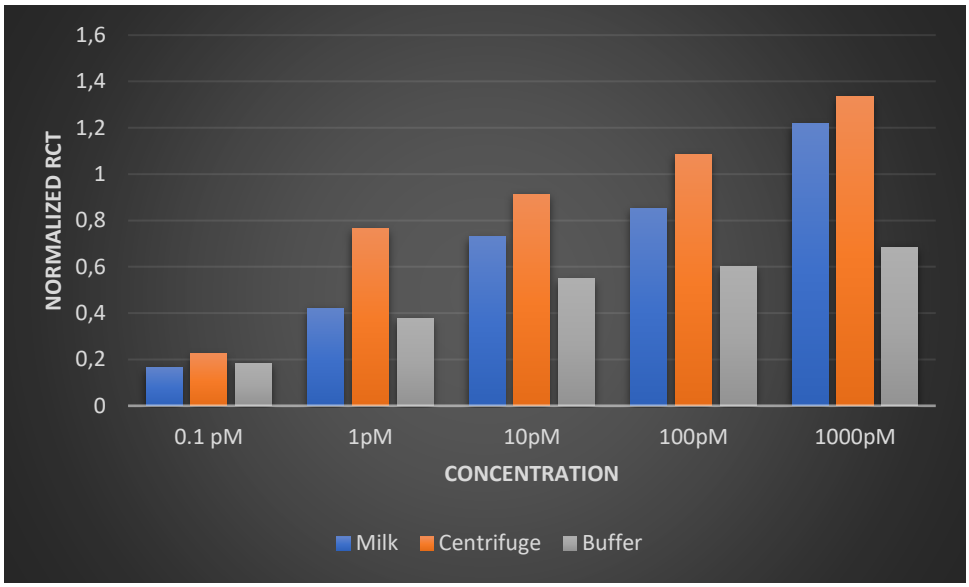

Figure 22.B. Bar chart comparing normalized Rct values against DNA concentrations obtained from EIS measurements using sensors prepared.

Lastly, the calibration curve obtained from SWV analysis using sensors tested in buffer, as shown in Figure 23.A, Figure 23.B, once again reflects a very similar pattern, given their neutral nature. As for the milk samples, firstly, the centrifuged milk experiences a linear and relatively stable decrease, confirming the validity of the pattern established in the previous EIS plots. In the case of the 0.1% milk sample, the current-related behavior decreases at a scaled and progressive rate, displaying a pronounced and significant reduction. This alignment with expectations once again corresponds with what was anticipated.

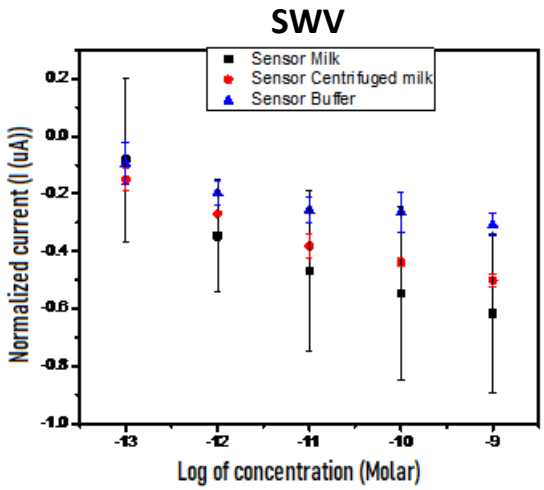

Figure 23.A. Detection obtained from SWV measurements performed between sensors.

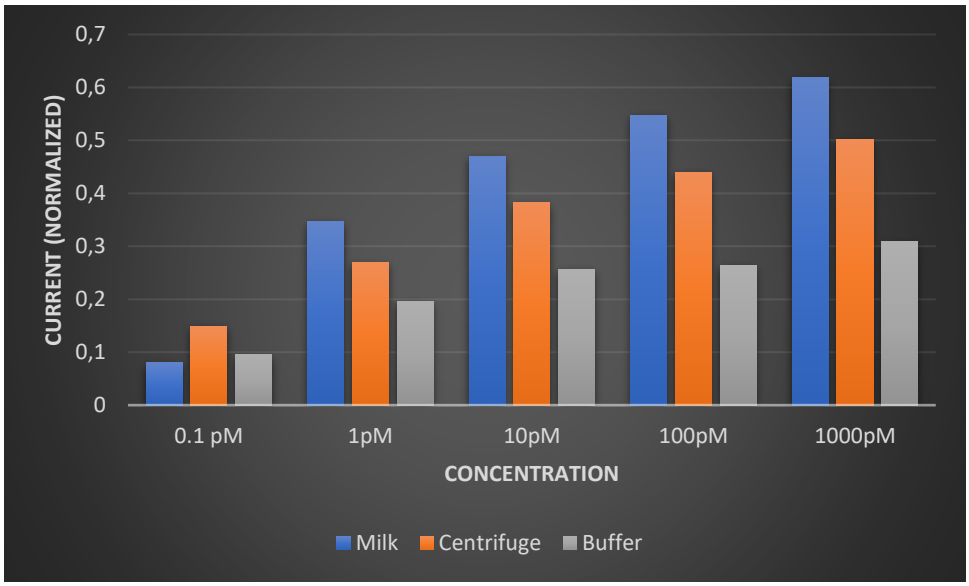

Figure 23.B. Bar chart comparing normalized Iox values against DNA concentrations obtained from SWV measurements using sensors prepared.

Lastly, the SWV analysis related to the sensor readings once again reflects a very similar pattern in the behavior of the buffer samples, given their neutral nature. As for the milk samples, firstly, the centrifuged milk experiences a linear and relatively stable decrease, confirming the validity of the pattern established in the previous EIS graph. In the case of the 0.1% milk sample, the current-related behavior decreases at a scaled and progressive rate, displaying a pronounced and significant reduction. This alignment with expectations once again corresponds with what was anticipated, a dcrease on the Iox values.

3. CONCLUSIONS.

The present work is focused around the optimization, modification, and subsequent utilization of a biosensor aimed at addressing therapeutic challenges in terms of mastitis bovine timely detection.

Understanding the underlying problem related to mammary gland inflammation, the current issue with late detection of bovine mastitis is rooted in the negative outcomes it brings. This includes lower quality and quantity of milk yield by affected cows, which repercutes economically on the dairy industry profitability and sustainability. Likewise, the overall health of the herd is also compromised. Like any contagious disease, if precautions aren't taken timely, the ailment can readily precipitate the dissemination, thereby amplifying the vulnerability of the herds. So, it's pretty clear that for this study's purpose, identifing the disease accurately in its early stages is imperative to minimize the detrimental aftermath that comes from it.

Biosensors are becoming increasingly prominent tools in the field of disease detection, as they facilitate rapid, sensitive, and highly accurate identification of analytes of interest. The process of miniaturization, coupled with advancements in electronics, has further enabled the creation of portable and cost-effective point-of-care testing. In our case, this advancement enables the on-site acquisition of milk samples promptly and with minimal invasiveness, which contributes to the livestock well-being.

In the context of our study, we embarked on the development of a biosensor with subsequent applications in electrochemical biodetection. It's noteworthy that the fabrication protocols employed throughout the process have been well-established, refined, and extensively studied. Consequently, many parameters have been optimized to achieve a more precise, reproducible and goal-oriented outcome. Thus, we were assured that the biosensor was a well-equipped tool for the pursuit of our objective. However, the experimental design did present certain challenges in interpreting the results of complex matrix, such as milk samples due to the inherent variability associated within different milk samples. Thereby, to assess matrix effects when testing milk and

studying different approaches to solve them. This variability arises from differences in nutritional composition, animal origin, physiological state, processing techniques, presence of residues and contaminants, as well as storage conditions. All these factors contribute to the slight divergence among milk samples, which is reflected in the result readings as significant divergence between samples of the same type and concentration, which leads to a lack of reproducibility in the samples. The problem that we wanted to adress relates then, to adress the complexity of any fresh sample, which contains a mixture of biomolecules prone to adsorb non-specifically on the sensor surface affecting the reliability of our measurements. However, all along the experiment we have worked with the same milk sample.

The obtained results, despite dealing with samples of great complexity, have allowed for consistent and reasonable outcomes. It has been observed that since incubating the milk sample one after another, the increase in the detection of the target mi-RNA molecule is linked to a rise in the exposed incubation time of the sample. The sensing process has been carried out through electrochemical detection, utilizing EIS and SWV methods. These methods employed Rct and Iox reading data, respectively, which were then graphically represented. MiRNA-223 sees elevated levels due to an immune response induced by inflammation-related bovine mastitis. It's important to differentiate results among the two types of samples used: 0.1% diluted milk and 0.1% diluted and centrifuged milk. This highlights the response in the absence of interfering species and the later assessing matrix effects work, and illustrates the function carried out by the centrifuge in separating solid components from liquids, which evidently conditions the results. These observations, in conclusion, have brought to light the process of passivation and have prompted us to consider the utilization of milk samples for surface blocking in other experimental processes. Highly effective passivation can serve as a valuable tool for conducting analytical analyses with the aim of enhancing or restricting undesirable interactions within the target sample. This is achieved through the application of a protective and stabilizing layer onto the sample's surface. This layer acts as a barrier to minimize further passivation and enhance reproducibility by reducing the variability resulting from unwanted interactions.

In response to escalating healthcare exigencies witnessed over the past few decades, a discernible necessity has emerged to channel resources into the development of high capacity and innovation biomedical projects. This imperative hinges upon harnessing advancements in technology to empower human capabilities and analytical acumen, thereby enabling the proficient formulation of accurate medical decisions, the expeditious establishment of reliable, preemptive diagnoses, and the execution of meticulous and personalized therapeutic interventions. Promt detection and point-of-care analysis of pathogens raises today challenges in tailoring appropiate treatment strategies and interventions to the present and future healthcare sector.

Lastly, addressing the importance of the use and development of personalized therapies, which allow delving into the unique requirements and needs of each person, both in the realm of human and animal medicine. Each individual possesses unique set of conditions and medical history that dictate their responses to environments, symptoms, treatments, and medical interventions. Tools need to be allocated to facilitate thorough, deep, and specific studies based on patient information, providing more accurate care and consequently significantly enhanced effectiveness. By achieving this, the personalization of treatment and diagnosis relies on the utilization of genetic studies and biomedical profiles, combined with the development of advanced diagnostic techniques, such as the designed pAAO biosensors. Those biosensors can achieve high sensitivity because of their large reactive surface area. They can also perform high sensitive analysis thereby using a specific sensing mechanism based on pore blockage, caused upon miRNA hybridization to the immobilized capture probe. And they can easily be modified according to the specific sensing requierements. PAAO-based biosensors aim to be a promising tool for timely disease detection, specifically designed for rapid, effective and on-site diagnosis, offering information that is subsequently used to study the behavior and response of inflammation due to bovine mastitis. The ultimate goal is to gather sufficient patient data, thereby permiting the development of unique and tailored treatments for each animal special needs.

Globally, efforts are being made to obtain early diagnostic tools for multiple urgent and concerning human diseases, using fluids such as sweat or plasma and their respective biomarkers. These tools aim to study the evolution, behavior, and spread of diseases in order to seek effective cures.

4. REFERENCES.

[1] Tzelos T, Ho W, Charmana VI, Lee S, Donadeu FX. MiRNAs in milk can be used towards early prediction of mammary gland inflammation in cattle. Sci Rep. 2022 Mar 24;12(1):5131. doi: 10.1038/s41598-022-09214-9. PMID: 35332227; PMCID: PMC8948199.

[2] Sharun, K., Dhama, K., Tiwari, R., Gugjoo, M. B., Iqbal Yatoo, M., Patel, S. K., Pathak, M., Karthik, K., Khurana, S. K., Singh, R., Puvvala, B., Amarpal, Singh, R., Singh, K. P., & Chaicumpa, W. (2021). Advances in therapeutic and managemental approaches of bovine mastitis: a comprehensive review. *The veterinary quarterly*, *41*(1), 107–136. https://doi.org/10.1080/01652176.2021.1882713

[3] Bradley A. (2002). Bovine mastitis: an evolving disease. *Veterinary journal (London, England : 1997)*, *164*(2), 116–128. https://doi.org/10.1053/tvjl.2002.0724

[4] Ruegg P. L. (2017). A 100-Year Review: Mastitis detection, management, and prevention. *Journal of dairy science*, *100*(12), 10381–10397. https://doi.org/10.3168/jds.2017-13023

[5] Condrat CE, Thompson DC, Barbu MG, Bugnar OL, Boboc A, Cretoiu D, Suciu N, Cretoiu SM, Voinea SC. miRNAs as Biomarkers in Disease: Latest Findings Regarding Their Role in Diagnosis and Prognosis. Cells. 2020 Jan 23;9(2):276. doi: 10.3390/cells9020276. PMID: 31979244; PMCID: PMC7072450

[6] Lai, Y. C., Fujikawa, T., Maemura, T., Ando, T., Kitahara, G., Endo, Y., Yamato, O., Koiwa, M., Kubota, C., & Miura, N. (2017). Inflammation-related microRNA expression level in the bovine milk is affected by mastitis. *PloS one*, *12*(5), e0177182. https://doi.org/10.1371/journal.pone.0177182

[7] Ashraf, A., & Imran, M. (2020). Causes, types, etiological agents, prevalence, diagnosis, treatment, prevention, effects on human health and future aspects of bovine mastitis. *Animal health research reviews*, *21*(1), 36–49. https://doi.org/10.1017/S1466252319000094

[8] What – biosensing bovine mastitis. (n.d.). https://www.biosensingbovinemastitis.com/what/

[9] Pyörälä S. (2003). Indicators of inflammation in the diagnosis of mastitis. *Veterinary research*, *34*(5), 565–578. https://doi.org/10.1051/vetres:2003026

[10] Menon, S., Mathew, M. R., Sam, S., Keerthi, K., & Kumar, K. G. (2020). Recent advances and challenges in electrochemical biosensors for emerging and re-emerging infectious diseases. Journal of electroanalytical chemistry (Lausanne, Switzerland), 878, 114596. https://doi.org/10.1016/j.jelechem.2020.114596

[11] Grieshaber, D., MacKenzie, R., Vörös, J., & Reimhult, E. (2008). Electrochemical Biosensors - Sensor Principles and Architectures. Sensors (Basel, Switzerland), 8(3), 1400–1458. https://doi.org/10.3390/s80314000

[12] Müsse, A., La Malfa, F., Brunetti, V., Rizzi, F., & De Vittorio, M. (2021). Flexible Enzymatic Glucose Electrochemical Sensor Based on Polystyrene-Gold Electrodes. Micromachines, 12(7), 805. https://doi.org/10.3390/mi12070805

[13] How – Biosensing bovine mastitis. (n.d.). https://www.biosensingbovinemastitis.com/how/

[14] Ravikumar, C., Wagassa, A. N., Ravikumar, C., & Nagaswarupa, H. (2022). Functionalized metal and metal oxide nanomaterial-based electrochemical sensors. In Elsevier eBooks (pp. 369–392). https://doi.org/10.1016/b978-0-12-823788-5.00001-6

[15] Santos, Dr. (2010). Structural Engineering of Nanoporous Anodic Alumina and Applications [Doctoral thesis]. Universitat Rovira i Virgili.

[16] Santos, A., Kumeria, T., & Losic, D. (2013). Nanoporous anodic aluminum oxide for chemical sensing and biosensors. Trends in Analytical Chemistry, 44, 25–38. https://doi.org/10.1016/j.trac.2012.11.007

[17] Naresh, V., & Lee, J. Y. (2021). A review on biosensors and recent development of Nanostructured Materials-Enabled biosensors. Sensors, 21(4), 1109. https://doi.org/10.3390/s21041109

[18] Gangwar, R., Ray, D., Rao, K. T., Khatun, S., Subrahmanyam, C., Rengan, A. K., & Vanjari, S. R. K. (2022). Plasma Functionalized Carbon Interfaces for Biosensor Application: Toward the Real-Time Detection of Escherichia coli O157:H7. ACS omega, 7(24), 21025–21034. https://doi.org/10.1021/acsomega.2c01802

[19] Martins, S. A. M., Martins, V. C., Cardoso, F. A., Germano, J., Rodrigues, M., Duarte, C., Bexiga, R., Cardoso, S., & Freitas, P. P. (2019). Biosensors for On-Farm Diagnosis of Mastitis. Frontiers in bioengineering and biotechnology, 7, 186. https://doi.org/10.3389/fbioe.2019.00186

[20] González-Sánchez, M., Gómez-Monedero, B., Agrisuelas, J., Iniesta, J., & Valero, E. (2018). Highly activated screen-printed carbon electrodes by electrochemical treatment with hydrogen peroxide. Electrochemistry Communications, 91, 36–40. https://doi.org/10.1016/j.elecom.2018.05.002

[21] Bakirhan, N. K. (2017). Sensitive and Selective Assay of Antimicrobials on Nanostructured Materials by Electrochemical Techniques. In Nanostructures for Antimicrobial Therapy. https://doi.org/10.1016/b978-0-323-46152-8.00003-2

[22] BioLogic. (2023b, August 9). What is CV? A comprehensive guide to Cyclic Voltammetry - BioLogic Learning Center. https://www.biologic.net/topics/what-is-cv-a-comprehensive-guide-to-cyclic-voltammetry/

[23] Venton, B. J., & DiScenza, D. J. (2020). Voltammetry. In Elsevier eBooks (pp. 27–50). https://doi.org/10.1016/b978-0-12-821203-5.00004-x

[24] Tolun, A., & Altintas, Z. (2023). Chemical sensing of food phenolics and antioxidant capacity. In Elsevier eBooks (pp. 593–646). https://doi.org/10.1016/b978-0-323-90222-9.00004-2

[25] Magar, H. S., Hassan, R. Y. A., & Mulchandani, A. (2021). Electrochemical Impedance Spectroscopy (EIS): Principles, Construction, and Biosensing Applications. Sensors (Basel, Switzerland), 21(19), 6578. https://doi.org/10.3390/s21196578

[26] Utec, B. (2022, January 5). ¿Qué es la espectroscopia de impedancia electroquímica? Medium. https://medium.com/@biomtis.peru/qu%C3%A9-es-la-espectroscopia-de-impedancia-electroqu%C3%ADmica-eb245997c818

[27] Mirceski, V., Skrzypek, S., & Stojanov, L. (2018). Square-wave voltammetry. ChemTexts, 4(4). https://doi.org/10.1007/s40828-018-0073-0

[28] Hoyos-Arbeláez, J., Vázquez, M. V., & Contreras-Calderón, J. (2017). Electrochemical methods as a tool for determining the antioxidant capacity of food and beverages: A review. Food Chemistry, 221, 1371–1381. https://doi.org/10.1016/j.foodchem.2016.11.017

[29] González-Sánchez, M., Gómez-Monedero, B., Agrisuelas, J., Iniesta, J., & Valero, E. (2018b). Highly activated screen-printed carbon electrodes by electrochemical treatment with hydrogen peroxide. Electrochemistry Communications, 91, 36–40. https://doi.org/10.1016/j.elecom.2018.05.002